


# Study of Protein Adsorption During Sterile Filtration of Protein Formulations by ILC

Susanne Maria Hilda Haindl<sup>1,2,\*</sup>, Olivia Doppleb<sup>1,3</sup>, Lucas Förster<sup>1,4</sup>, Sophia Wraage<sup>1</sup>, and Annette Reiche<sup>1</sup>

DOI: 10.1002/cite.201900185

 This is an open access article under the terms of the Creative Commons Attribution License, which permits use, distribution and reproduction in any medium, provided the original work is properly cited.

Protein adsorption is usually regarded as the main reason for filter fouling in sterile filtration of protein formulations. To achieve a better insight into this phenomenon, protein adsorption was studied during filtration of stabilized bovine serum albumin (BSA) and  $\gamma$ -globulin formulations through 0.2- $\mu\text{m}$  microfilter membranes by inverse liquid chromatography (ILC). Adsorption processes can be studied with this method by measurement of breakthrough curves. The change of the concentration in the fluid phase is measured with high accuracy by an inline UV-detector.

**Keywords:** Inverse liquid chromatography, Protein adsorption, Sterile filtration

*Received:* December 16, 2019; *revised:* April 02, 2020; *accepted:* May 22, 2020

## 1 Introduction

Biopharmaceuticals are drugs produced from biological sources. Usual drug products can be described as a colloidal dispersion of a therapeutic active protein in an aqueous buffered solution containing further excipients, e.g., surfactant, sugars or amino acids. These excipients stabilize the protein, i.e., increase physical and chemical stability and prevent aggregation, adsorption or denaturation. [1, 2]

The biopharma process chain for drug production is a long and complex multistep process for cultivation, harvesting and purification of proteins. It contains many microfiltration steps for bioburden reduction and sterile filtration. In course of the production process, protein solutions are buffered only according to production requirements and not to gain maximum stability. [3]

Interaction with the filter can cause filter fouling and product loss. Therefore, low adsorptive filter properties are a requirement for suitability of filter products for filtration of protein formulations. Aim of this work is the establishment of a reliable method to study adsorption during microfiltration processes. An inverse liquid chromatography system (ILC) was used to perform both, filtration and adsorption measurement. Adsorption can be studied by UV detection of the protein concentration in the filtrate.

Methods to study adsorption phenomena at surfaces by measurement and analysis of breakthrough curves have been frequently described in literature [4–6]. Those measurements can be performed in principle with commercially available Äkta test equipment. However, the equipment and experimental approach used in this study was optimized to examine low and unspecific adsorption in course of microfiltration. The experimental procedures, data evaluation and

calculation basis are described. Furthermore, important impact factors on protein adsorption during filtration were studied, e.g., formulation ingredients, protein concentration, membrane type, and the filtration flow rate.

The study focuses on protein adsorption from stabilized protein formulations, i.e., formulations with a low degree of aggregation due to choice of pH value and addition of a surfactant (PS80). Adsorption was investigated for filtration through cellulose nitrate membranes and cellulose membranes (Hydrosart<sup>®</sup>). These membranes have been selected to study membranes with contrary surface properties. Cellulose nitrate membranes have hydrophobic surface properties and are known for their high protein binding capacity. Contrary, Hydrosart membranes, i.e., crosslinked cellulose membranes, are materials with low protein binding capacity due to their hydrophilic surface properties.

<sup>1</sup>Susanne Maria Hilda Haindl, Olivia Doppleb, Lucas Förster, Sophia Wraage, Dr. Annette Reiche  
susanne.haindl@sartorius-stedim.com  
Sartorius Stedim Biotech GmbH, August-Spindler-Straße 11, 37089 Göttingen, Germany.

<sup>2</sup>Susanne Maria Hilda Haindl  
Leibniz-Universität Hannover, Institut für Technische Chemie, Callinstraße 5, 30167 Hannover, Germany.

<sup>3</sup>Olivia Doppleb  
Clausthal University of Technology, Institut für Physikalische Chemie, Arnold-Sommerfeld-Straße 4, 38678 Clausthal-Zellerfeld, Germany.

<sup>4</sup>Lucas Förster  
Georg-August-Universität Göttingen, Institut für Organische und Biomolekulare Chemie, Tammannstraße 2, 37077 Göttingen, Germany.

## 2 Theoretical Background

Adsorption processes are usually described by the Langmuir theory, which was originally developed to describe the adsorption of gases. The theory assumes that (I) only a monomolecular layer adsorbs (II) reversibly to a (III) homogeneous smooth surface with equivalent binding sites B. The molecules M do not interact with each other upon adsorption:  $M + B \rightleftharpoons MB$ .

The surface coverage  $\theta$  can be described by the solute concentration  $c$ , and a constant  $K$ .

$$\theta = \frac{Kc}{1 + Kc} \quad (1)$$

The constant  $K$  is defined by the rate constant  $k_{ad}$  for the adsorption and the rate constant  $k_{de}$  for the desorption step:

$$K = \frac{k_{ad}}{k_{de}} \quad (2)$$

The Langmuir theory is quite frequently used for description of protein adsorption [7–12], although, the three basic theoretical requirements mentioned above usually do not fit. Adsorption sites are not uniform in size and energy and protein aggregation can lead to the adsorption of multilayers. Furthermore, protein adsorption is a process with multiple steps involving structural rearrangements at the surface and a full surface coverage can be obtained with different protein loadings [13–15]. Finally, protein adsorption can lead to irreversible coverage of the surface [16]. Therefore, modifications of the Langmuir theory are necessary to describe protein adsorption.

Another way to describe adsorption is the Brunauer, Emmet and Teller (BET) theory. The concept is based on the assumption that additional adsorption can occur at an already adsorbed monolayer. Here, every adsorbed molecule can be a possible adsorption site for the next. The adsorbed amount of solute  $L$  for a monolayer  $L_{mono}$ , the solute concentration  $c$  and the constant  $z$  for a given concentration are described by Eq. (3).

$$\frac{L}{L_{mono}} = \frac{cz}{(1-z)\{1-(1-c)z\}} \quad (3)$$

For the BET adsorption isotherm, the constant  $z$  is defined by Eq. (4):

$$z = \frac{c}{c^*} \quad (4)$$

The concentration  $c^*$  is the concentration needed to achieve a surface coverage of more than a monolayer.

Langmuir and BET adsorption isotherms are presented in Fig. 1. It can be seen that for the Langmuir isotherm, the surface coverage approaches a limiting value. The BET adsorption isotherm reaches a plateau at monolayer coverage and continues at an increasing slope.

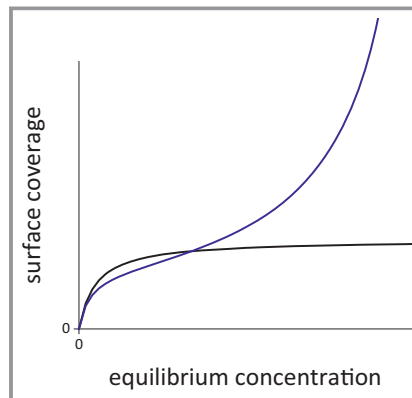


**Figure 1.** Comparison of Langmuir adsorption isotherm (black), and BET adsorption isotherm (blue).

Further models were developed for the description of protein adsorption kinetics. Most models expand the classical Langmuir model by one or more reactions that can occur at the interface (conformational changes or flocculation). The two-state model for example can be used to describe adsorption processes including conformational changes, dimerization processes or denaturation (Fig. 2).

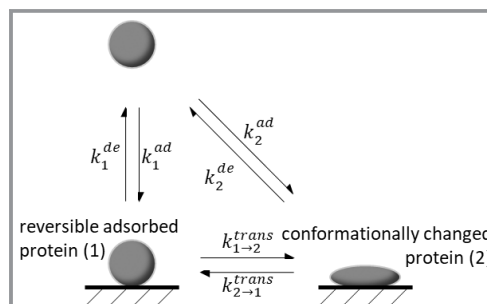


**Figure 2.** Schematic presentation of the two-state model for reversible protein adsorption.

To describe the adsorption equilibrium at the interface for two different states, the following equations are needed:

$$\frac{d\theta_1}{dt} = k_1^{ad} c \Phi(\Theta) - k_1^{de} \Theta_1 - k_{1 \rightarrow 2}^{trans} \Theta_1 + k_{2 \rightarrow 1}^{trans} \Theta_2 \quad (5)$$

$$\frac{d\theta_2}{dt} = k_2^{ad} c \Phi(\Theta) - k_2^{de} \Theta_2 - k_{2 \rightarrow 1}^{trans} \Theta_2 + k_{1 \rightarrow 2}^{trans} \Theta_1 \quad (6)$$

The surface coverage of the respective states are calculated by the adsorption and desorption rate  $k_n^{ad}$  and  $k_n^{de}$  of state 1 and 2, the concentration in the bulk solution and the respective surface coverages  $\Theta_n$  of state 1 and 2. The transition of state 1 and 2 and of state 2 to state 1 are included by the rate constants  $k_{1 \rightarrow 2}^{trans}$  and  $k_{2 \rightarrow 1}^{trans}$ .

$\Phi(\Theta)$  is called the available surface function (Eq. (7)) and is part of the random sequential adsorption model. It

accounts to the fact that proteins can only adsorb to surface sites that are not occupied by another protein. If a protein approaches a site that is (partially) occupied by another protein, it is rejected and does not adsorb. Adsorption is assumed to be an irreversible process, and the molecules cannot diffuse on the surface. [17, 18]

$$\Phi(\theta) = \frac{\left(1 - \frac{\theta}{\theta_i}\right)^3}{1 - 0.812\left(\frac{\theta}{\theta_i}\right) + 0.2336\left(\frac{\theta}{\theta_i}\right)^2 + 0.0845\left(\frac{\theta}{\theta_i}\right)^3} \quad (7)$$

As we expect at least partial adsorption, the random sequential adsorption model might not work.

In this work, the adsorption of proteins during filtration of bovine serum albumin (BSA) and  $\gamma$ -globulin are examined. Both proteins are so-called soft proteins; soft proteins adsorb on every surface and change in conformation because of a conformational entropy gain. Desorbed proteins tend to adsorb even better. [7]

For a complete mechanistic understanding, every single elementary reaction should be considered. However, this was not possible with the available equipment. Therefore, it was decided that only the macroscopic effects are described and not all the single elementary reactions. All the adsorption and desorption reactions are described by their total. Furthermore, it is examined how much protein is irreversibly bound to the interface due to multiple site adsorption or conformational changes. To achieve this goal, the two-state model can be used. By turning state 2 to an irreversible adsorbed protein, Eqs. (5) and (6) are simplified:

$$\frac{d\theta_1}{dt} = k_1^{\text{ad}} c \Phi(\theta) - k_1^{\text{de}} \theta_1 - k_{1 \rightarrow 2}^{\text{trans}} \theta_1 \quad (8)$$

$$\frac{d\theta_2}{dt} = k_2^{\text{ad}} c \Phi(\theta) + k_{1 \rightarrow 2}^{\text{trans}} \theta_1 \quad (9)$$

## 2.1 Inverse Liquid Chromatography

The ILC is a chromatographic method used for the examination of the adsorption of molecules from a fluid phase to a stationary phase by measurement of breakthrough curves. In this work the ILC (setup shown in Fig. 3) is used to study the adsorption of proteins on the surface of a membrane during filtration of protein formulations (fluid phase) through microfilter membranes with 0.2  $\mu\text{m}$  nominal pore size (stationary phase).

With this method it is possible to investigate adsorption thermodynamics and kinetics in an automated way. It can be seen whether the adsorption is reversible or not and the adsorption rate can be determined. Experimental details, data evaluation and calculation basis are described in the following section.

The ILC presented in Fig. 3 was configured with 14 measurement places in collaboration between Sartorius Stedim Biotech GmbH and Knauer Wissenschaftliche Geräte GmbH. All tubing of the chromatography setup is made of stainless steel and with identical length for minimum adsorption and prevention of contamination.

The filtration flow rate can be adjusted from 0.15 to 10  $\text{mL min}^{-1}$  (16 LMH–1097 LMH). In all experiments a fixed volume of 40 mL of test fluid was used for the

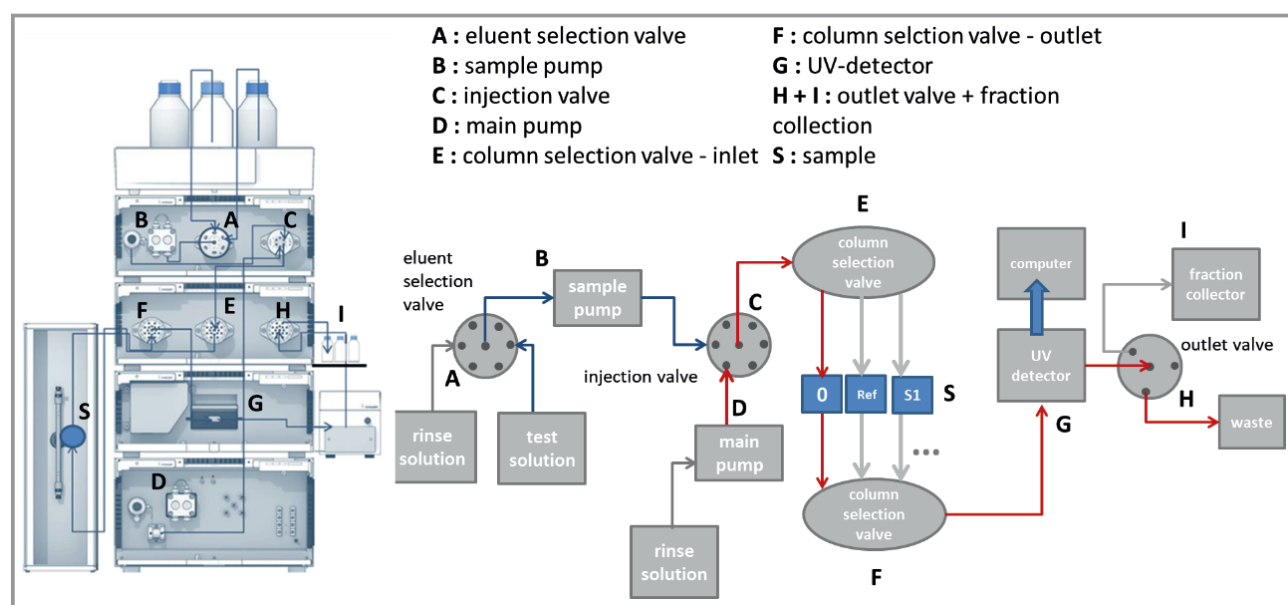


**Figure 3.** Setup of inverse liquid chromatography (configured by Sartorius Stedim Biotech GmbH und Knauer; picture reprinted with permission from Knauer Knauer Wissenschaftliche Geräte GmbH).

measurement. This amount was determined in previous experiments as necessary to ensure an adsorption equilibrium.

Adsorption and desorption processes can be studied by pumping first test fluid then buffer solution through the sample. For multiple measurement cycles consisting of an adsorption and a desorption step the setup was flushed with 40 mL of test solution and 30 mL buffer solution each cycle.

Breakthrough curves were monitored by measurement of the protein concentration of the filtrate by UV detection. Four different UV wavelengths can be collected simultaneously every 0.001 min, independent of the filtration flow rate. A wavelength of 280 nm was chosen for the data analysis, as for this wavelength protein concentration was linear with signal intensity in the concentration range of  $1 \text{ g L}^{-1}$  to  $5 \text{ g L}^{-1}$  BSA, which was not the case for 195 nm, 230 nm, and 240 nm.

Measurements were performed in filter holders made from low adsorptive Cyrolite<sup>®</sup> (Fig. 4). Single layer 30-mm membrane discs with  $5.52 \text{ cm}^2$  of effective membrane area were used for the measurements. The resulting breakthrough curve for a membrane in the filter holder contains information about adsorption of the system, the filter holder and the membrane. Therefore, separate breakthrough curves of the system blank, the empty filter holder and the filter holder with membrane (sample measurements) are required for calculation of protein adsorption on the membrane surface. The adsorption of the filter holder is substantial. It was determined by measurement of a high number of breakthrough curves for the empty filter holder for every protein formulation, and the adsorbed amount of protein to the membrane housing was calculated by averaging the results of at least six measurements.

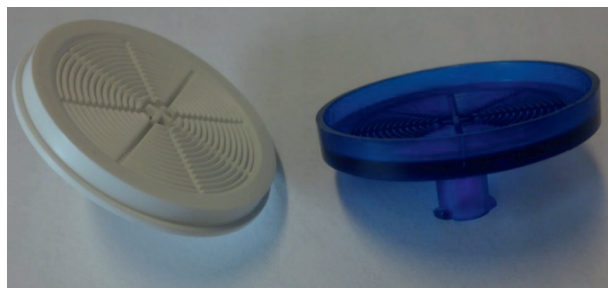


Figure 4. Cyrolite<sup>®</sup> membrane housing for ILC measurements.

### 2.1.1 Assembly and Operation of the ILC

At first the membranes are installed in the membrane housings. The Hydrosart membrane is wetted spontaneously and swells upon water contact, therefore, this membrane is installed dry. The cellulose nitrate membrane is prewetted with the respective buffer solution.

All measurements were performed in an automated way. After setup assembly, air is removed out of the system by

flushing with water, then the ILC is preconditioned with protein buffer. After the respective measurement position the ILC is flushed with buffer, the sample valve switches to the test solution. 40 mL test solution are applied with the predefined flow rate (usually  $0.9 \text{ mL min}^{-1} \text{ cm}^{-2}$ ) under monitoring of the change of the UV signal. Then the sample valve is switched to the buffer solution once again, and desorption process can be monitored. Between measurement trials the setup is flushed with a cleaning solution (1 % sodium dodecyl sulfate and 0.1 M sodium hydroxide) for complete protein removal.

Furthermore, repeated measurement cycles of alternating sample and buffer injection are performed in order to see the influence of pre-adsorbed protein layers on protein adsorption. The influence of this pre-adsorbed layer on further adsorption measurements is examined by measuring a total of five adsorption-desorption cycles.

### 2.1.2 Data Analysis

Every 0.001 min a data point was recorded, consequently the amount of data points depends on the filtration flow rate. Fig. 5 shows a typical ILC measurement curve. For data evaluation, first data reduction to 13 000 data points was performed. Afterwards, the breakthrough point of the buffer solution at the end of the breakthrough curve (Fig. 5) was determined manually. The starting point of each measurement was calculated based on this breakthrough point with the sample volume and the filtration flow rate (Fig. 5). This method was established in order to eliminate errors that occur in case of a theoretically possible complete protein adsorption at the beginning of a measurement. In literature, usually the first initial rise of the UV signal is taken. [6]

With a distance of  $-10$  data points to the determined breakthrough point the UV intensity values of 10 data points were averaged and taken as equal to the initial sample concentration. Based on this, the concentration of the protein formulation can be calculated from the measurement curves according to Beer's law and the linear relationship between the intensity signal and the protein concentration.

The adsorbed amount of protein is calculated by integration of the breakthrough curves of blank, empty membrane housing and measurement run and subtraction of the resulting values as summarized schematically in Fig. 5b (green area).

A further complication arises from the different fluid flow of empty filter holders and filter holders filled with a membrane. This leads to a deformation of the adsorption curve of the empty filter holder. To solve this problem, first the adsorbed amount of protein to the empty filter holder is calculated. For this the area between the system blank concentration curve and the concentration curve of the empty filter holder is integrated and the adsorbed amount of protein at 40 mL sample solution is calculated. For the adsorption to the membranes, the area between the system blank

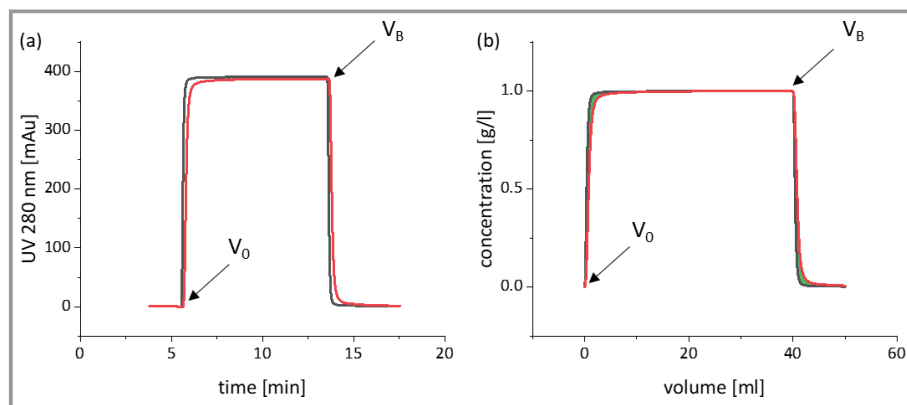


**Figure 5.** Data analysis of an ILC experiment. Measurement curve (a) and calculated concentration curve (b) for system blank (black) and membrane sample (red). Indicated are the break-through point of buffer solution ( $V_B$ ) and the calculated onset of protein sample ( $V_0$ ). The adsorbed amount of protein is calculated by integrating the area between the two concentration curves (green).

concentration curve and the membrane concentration curve is calculated again. Afterwards the adsorption curve is expanded by a correction factor  $CF$  to eliminate the amount of protein adsorbed to the membrane housing. The reference point for the expansion of the curve is at 40 mL test solution for the adsorbed amount of protein to the membrane material  $m_{\text{ads}@40\text{mL,membrane}}$  and the membrane housing  $m_{\text{ads}@40\text{mL,housing}}$ .

$$CF = \frac{m_{\text{ads}@40\text{mL,membrane}} - m_{\text{ads}@40\text{mL,housing}}}{m_{\text{ads}@40\text{mL,membrane}}} \quad (10)$$

With the adsorbed amounts of protein  $m_{\text{ads}}$  the adsorption rate was calculated by the following equation:

$$\text{adsorption rate} = \frac{dm_{\text{ads}}}{dt} \quad (11)$$

In this context desorption can be observed as a negative adsorption rate.

### 2.1.3 Membrane Materials

A cross-linked membrane of regenerated cellulose (Hydrosart) and a cellulose nitrate membrane were used for measurements, both with 0.2  $\mu\text{m}$  nominal pore size. The properties of the membranes are presented in Tab. 1.

### 2.1.4 Preparation of the Test Solution

Reverse osmosis water is used for preparation of the buffer solution. For preparation of the test solution lyophilized proteins are added slowly to the buffer solution under stirring. BSA was obtained by Kraeber & Co KG (order number 04180 10900) and  $\gamma$ -globulin by Merck KGaA (order number G5009).

The buffer solutions are stirred slowly with a magnetic stirrer. All solutions (reverse osmosis water, buffer, test solution and cleaning solution) are prefiltered with a 0.2- $\mu\text{m}$  Sartolab polyethylene sulfone filter and degassed. The composition of the test solution was varied between trials to examine formulation influences. The solution compositions are presented in Tabs. 2 and 3.

## 3 Results

### 3.1 System and Membrane Adsorption

Protein adsorption on the filter holder material was found to be substantial. Reliable results could only be obtained using filter housings with 4.5  $\text{cm}^2$  membrane area made from low adsorptive Cyrolyte<sup>®</sup>. Even then, protein adsorption is in the range of  $420 \pm 50 \mu\text{g}$  for the filter housing and  $15 \pm 10 \mu\text{g cm}^{-2}$  for membrane material (conditions: flow rate of 0.9  $\text{mL min}^{-1}\text{cm}^{-2}$  and protein concentration of 1  $\text{g L}^{-1}$ , formulation containing more than 0.01 % PS80). Protein adsorption to the filter holder grows proportional to the protein concentration in the formulation but was quite independent of the type of protein studied, the presence of surfactant in the protein formulation, and the filtration flow rate.

It was tried to improve the ratio between membrane and housing adsorption by using several layers of membrane in

**Table 1.** Properties of Hydrosart and cellulose nitrate membranes.

Membrane	Hydrosart	Cellulose nitrate
Material properties	hydrophilic	hydrophobic
Water flow rate [ $\text{mL cm}^{-2}\text{min}^{-1}\text{bar}^{-1}$ ] <sup>a)</sup>	18.4	20.4
Bubble point [bar] <sup>a)</sup>	3.40	4.40
Mean flow pore size [ $\mu\text{m}$ ] <sup>a)</sup>	0.52	0.44
BET surface [ $\text{m}^2\text{g}^{-1}$ ] <sup>b)</sup>	4.20	11.10
Porosity [%]	64	75
Weight [ $\text{g m}^{-2}$ ] <sup>b)</sup>	82.4	54.8
Thickness [ $\mu\text{m}$ ] <sup>c)</sup>	154	131
BET · Weight [ $\text{m}^2\text{m}^{-2}$ ]	346	608

a) Measurement with RO water; b) measurement with dried membranes; c) Measurement under ambient conditions; other values calculated.



**Table 2.** Compositions of the different BSA test formulations and filtration conditions for ILC measurements.

Trial	BSA concentration [g L <sup>-1</sup> ]	PS80 concentration [%]	Flow rate [mL min <sup>-1</sup> cm <sup>-2</sup> ]	Buffer & additives
Standard composition A	1	0.01	0.90	100 mM NaH <sub>2</sub> PO <sub>4</sub> , 100 mM Na <sub>2</sub> SO <sub>4</sub> , pH 6.9 0.01 % NaCl, 0.002 % NaN <sub>3</sub> , pH adjusted with NaOH
PS80 test series	1	0, 1.6 · 10 <sup>-4</sup> , 0.01, 0.5		
Variation of protein concentration	0.1, 0.5, 1.0, 2.0, 5.0	0.01		
Multiple cycles	1	0, 0.01		

**Table 3.** Compositions of the different  $\gamma$ -globulin test formulations and filtration conditions for ILC measurements.

Trial	$\gamma$ -globulin concentration [g L <sup>-1</sup> ]	PS80 concentration [%]	Flow rate [mL min <sup>-1</sup> cm <sup>-2</sup> ]	Buffer & additives
Standard composition B	1	0.01	0.90	75 mM histidine, pH 6.4, 0.002% NaN <sub>3</sub> , pH adjusted with HCl
PS80 test series	1	0, 0.01	0.90	
Variation of protein concentration	0.1, 0.5, 1.0, 2.0, 5.0	0.01	0.90	
Flow rate series	1	0.01	0.18, 0.45, 0.90, 1.41	
Multiple cycles		0	0.90	

the filter holder. Surprisingly, it was found that protein adsorption is proportional to the active filter area only and not to the total area of membrane placed in the membrane housing. It gives first impression of the complex nature of protein adsorption. Furthermore, it can be concluded that protein adsorption is focused on the contact area between membrane surface and fluid phase and that proteins are not homogeneously covered over the membrane surface area.

### 3.2 Influence of Surfactant (PS80) on Protein Adsorption

Filtration trials were performed with formulations with protein concentration of 1 g L<sup>-1</sup> at a flow rate of 0.9 mL min<sup>-1</sup>cm<sup>-2</sup> to assess the influence of the surfactant PS80 on protein adsorption to the membrane surface. The surfactant concentration was varied between 0 and 0.5 % PS80. PS80 has a critical micelle concentration (CMC) of 0.001 %. [19] The measured adsorption curves are presented in Fig. 6.

As already discussed, equilibration state was reached for all measurements under the chosen experimental conditions.

Protein adsorption on Hydrosart membranes was always minimal, in the range of 25  $\mu\text{g cm}^{-2}$ , independent of the

surfactant concentration. The surfactant has a low influence. However, protein adsorption on hydrophobic CN membranes depends strongly on the surfactant concentration. For formulations with a PS80 concentration above the CMC (0.01 % and 0.5 % PS80), a behavior comparable with that described for protein adsorption on hydrophilic surfaces was observed.

For formulations with a PS80 concentration below the CMC a distinctly higher protein adsorption was measured. For BSA, values around 100–150  $\mu\text{g cm}^{-2}$  were measured and in case of  $\gamma$ -globulin 160–200  $\mu\text{g cm}^{-2}$ , respectively. Interestingly, less adsorption was obtained for the surfactant-free BSA formulation compared with a formulation containing 0.00016 % PS80. Maybe the presence of the surfactant enables the protein to pack more closely on the surface. In literature it is described as well that the pre-exposure of hydrophobic surfaces with PS80 can reduce protein adsorption significantly [2, 16].

### 3.3 Protein Adsorption and Desorption – Multiple Measurement Cycles

Multiple adsorption and desorption cycles were measured in order to examine the reversibility of adsorption and desorption and the influence of pre-adsorbed protein molecules on the membrane surface on adsorption of further protein. Measurements were performed with surfactant-free protein formulations and formulations containing 0.01 % PS80, always with a protein concentration of 1 g L<sup>-1</sup> and at a filtration flow rate of 0.9 mL min<sup>-1</sup>cm<sup>-2</sup>. Fig. 7 presents results for the surfactant containing BSA formulations. In accordance with the results described above, adsorption is always in the range of 10–25  $\mu\text{g cm}^{-2}$ , independent of measurement cycle and type of membrane material. Adsorption is reversible.

Fig. 8 presents the results for the surfactant-free BSA and  $\gamma$ -globulin formulations. Additionally, adsorption and desorption rates for the multiple measurement cycles for BSA and  $\gamma$ -globulin are shown in Fig. 9. Adsorption and desorption rates for the multiple measurement cycles presented in Fig. 8 for PS80-free BSA (a and c) and  $\gamma$ -globulin (b and d) formulations. Adsorption and desorption rates

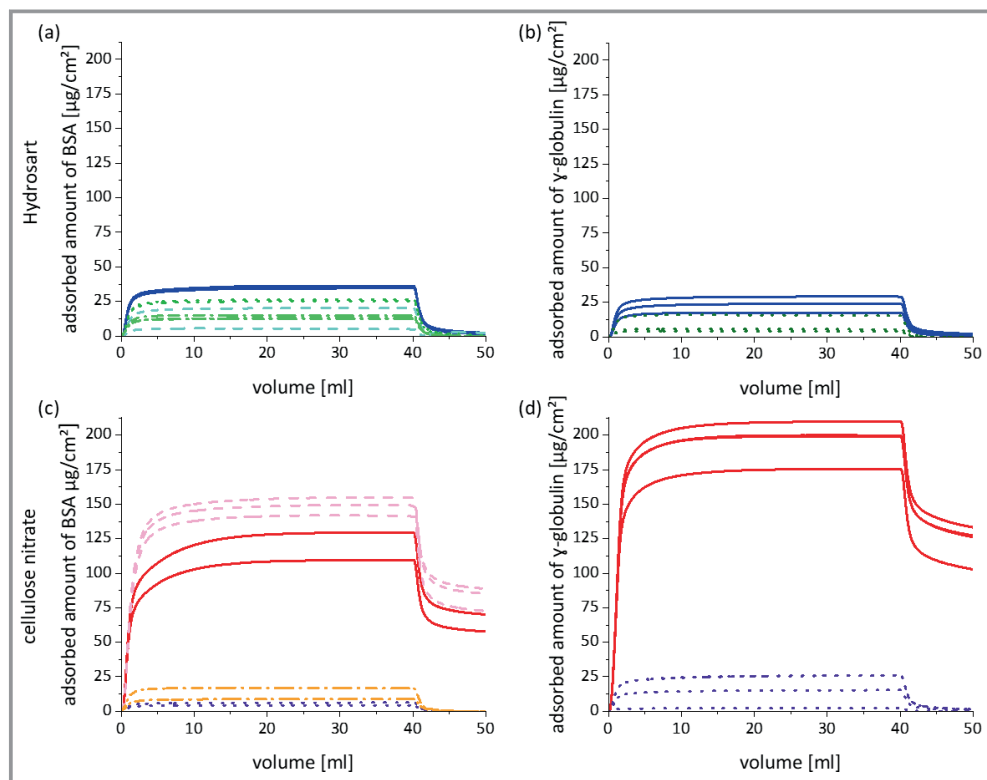


**Figure 6.** Adsorption of BSA (a and c) and  $\gamma$ -globulin (b and d) during filtration of protein formulations containing a different amount of PS80 through Hydrosart (a and b) and CN membranes (c and d). Formulation and process conditions are given in Tabs. 2 and 3. 0 % PS80 (blue and red, straight lines),  $1.6 \cdot 10^{-4}$  % PS80 (cyan and rose, dashed lines), 0.01 % PS80 (olive and lilac, dotted lines) and 0.5 % PS80 (green and orange, dotted and dashed lines).

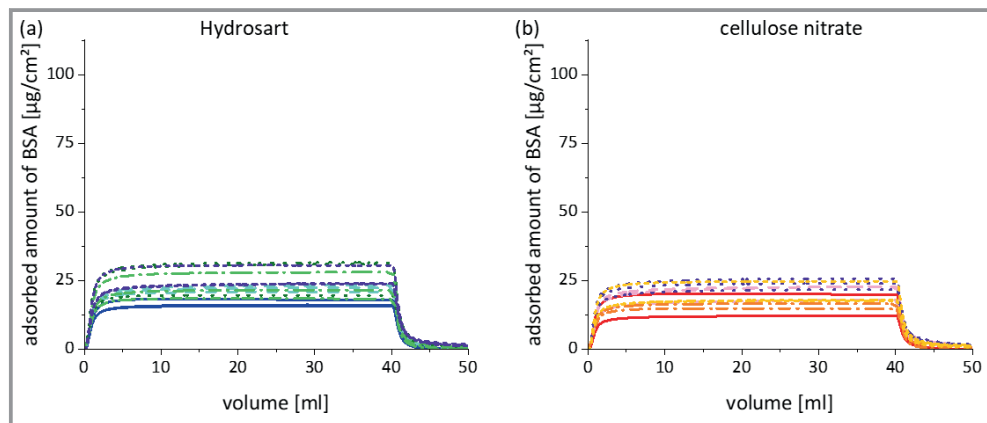


**Figure 7.** Adsorption of BSA during filtration of BSA formulations containing 0.01 % PS80 (formulation and process conditions in Tab. 2) in course of multiple adsorption and desorption cycles. a) Hydrosart and b) CN membrane; 1st measurement cycle (blue and red, straight lines), 2nd measurement cycle (cyan and rose, dashed lines), 3rd measurement cycle (olive and lilac, dotted lines), 4th measurement cycle (green and orange, dotted and dashed lines) and 5th measurement cycle (lilac and yellow, short dashed lines).

are calculated according to Eq. (11). Protein adsorption on hydrophilic Hydrosart membranes is again in the range of  $10\text{--}25 \mu\text{g cm}^{-2}$  and reversible.

A different behavior is observed for adsorption on hydrophobic CN membranes. Very strong adsorption was measured for the first measurement cycle for BSA (up to  $100 \mu\text{g cm}^{-2}$ ) and for  $\gamma$ -globulin (up to  $200 \mu\text{g cm}^{-2}$ ). In the

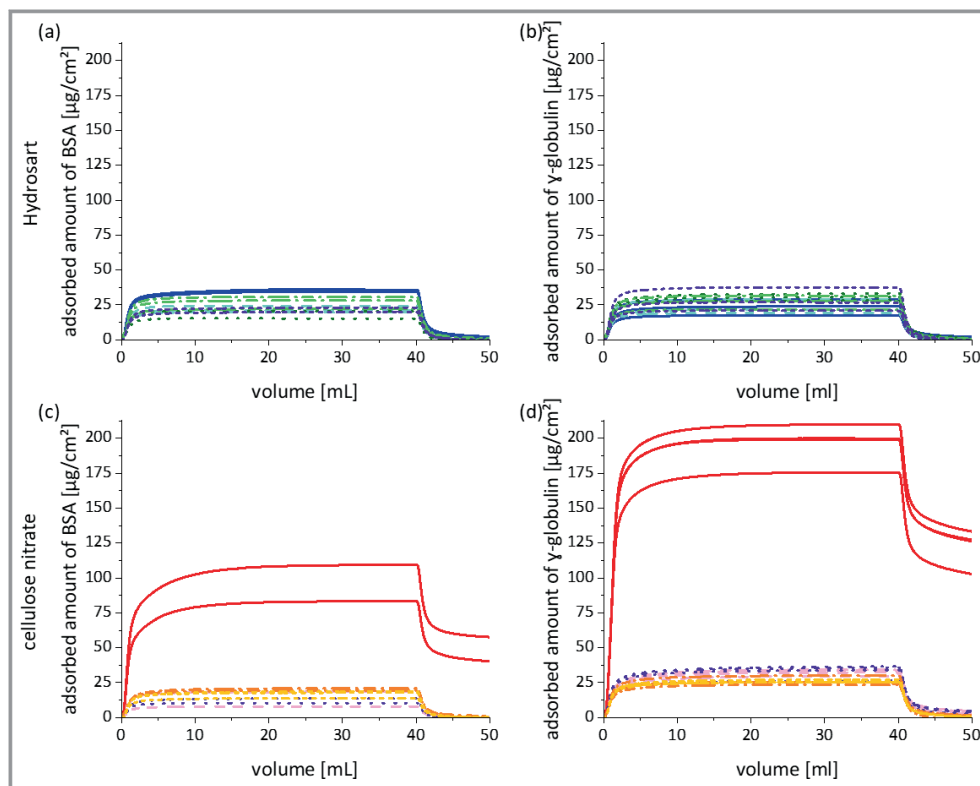


**Figure 8.** Adsorption of BSA (a and c) and  $\gamma$ -globulin (b and d) during filtration of PS80-free protein formulations (formulation and process conditions in Tabs. 2 and 3) in course of multiple adsorption and desorption cycles. a,b) Hydrosart and c,d) CN membrane; 1st measurement cycle (blue and red, straight lines), 2nd measurement cycle (cyan and rose, dashed lines), 3rd measurement cycle (olive and lilac, dotted lines), 4th measurement cycle (green and orange, dotted and dashed lines) and 5th measurement cycle (lilac and yellow, short dashed lines).

following desorption process only parts of the adsorbed protein can be removed by flushing with the buffer solution, which clearly indicates that protein adsorption was partly irreversible. For all following adsorption and desorption processes again reversible behavior was observed with adsorption in the range of  $10\text{--}25\ \mu\text{g cm}^{-2}$ .

Fig. 9 illustrates that protein adsorption on Hydrosart is reversible (hysteresis can be observed). Adsorption and desorption rates are comparable for all measurement cycles. Maximum adsorption and desorption rates are in the range of  $150\ \mu\text{g cm}^{-2}\text{min}^{-1}$ .

For the CN membrane it can be seen that the adsorption rate for the first cycle is highly increased. For BSA the adsorption rate declines rather fast, whereas it stays on a high level for  $\gamma$ -globulin before the decline. The adsorption rates in the following measurement cycles are distinctly lower and on the same level as for the Hydrosart membrane material ( $150\ \mu\text{g cm}^{-2}\text{min}^{-1}$ ). Desorption rates for the CN membrane are in the first cycle elevated compared to the following cycles, but the difference is not as distinct as for the adsorption rate. Another effect that can be seen quite well is that the protein desorption is not complete on CN in the first measurement cycle.

The results show that protein adsorption on hydrophobic membranes in the absence of PS80 is very strong and mechanistically complex. It is concluded that in the first measurement cycle protein sticks to the hydrophobic CN material irreversibly and turns the surface hydrophilic. Further protein adsorption in following measurement cycles is reversible and can be compared with adsorption on hydrophilic Hydrosart membranes concerning adsorption level and adsorption rate.

The results here are in agreement with literature. Here it is described as well that pre-exposure of surfaces with BSA can significantly reduce protein adsorption [20].

### 3.4 Influence of Filtration Flow Rate on Protein Adsorption

Measurements were performed for stabilized BSA and  $\gamma$ -globulin formulations containing 0.01 % PS80. Flow rates were varied between  $0.5\ \text{mL min}^{-1}$  and  $7.5\ \text{mL min}^{-1}$ . Protein adsorption was always in the range of  $20\text{--}30\ \mu\text{g cm}^{-2}$  independent of the flow rate. No significant differences can be observed for protein adsorption in the measurement



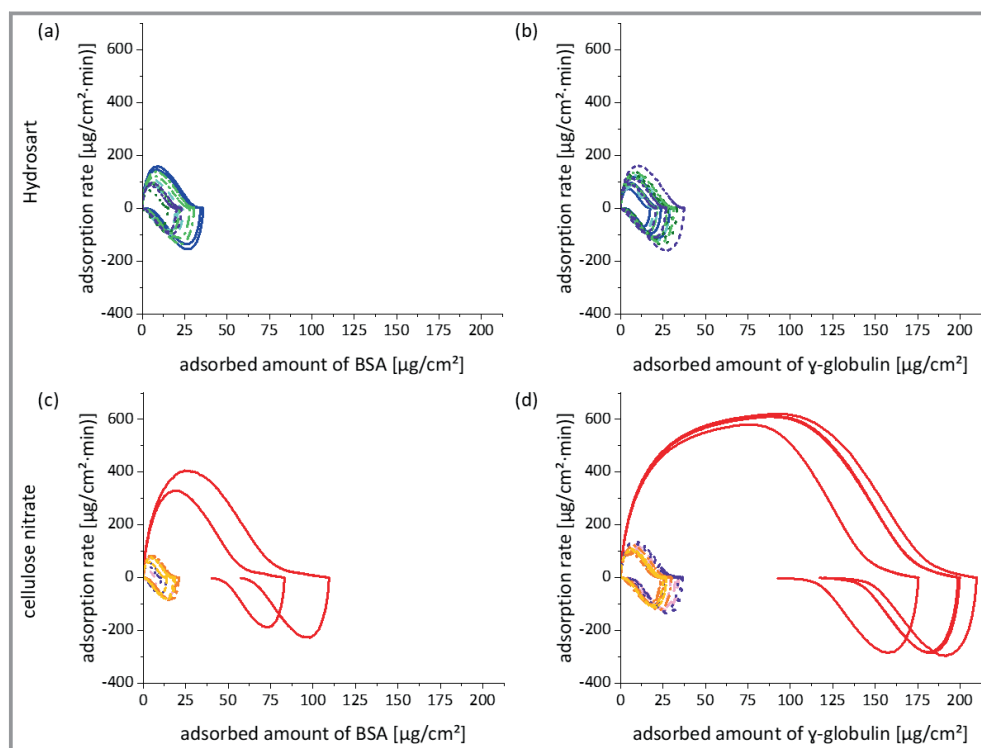


**Figure 9.** Adsorption and desorption rates for the multiple measurement cycles presented in Fig. 8 for PS80-free BSA (a and c) and  $\gamma$ -globulin (b and d) formulations. Description as in Fig. 8.

range of  $1 \text{ mL min}^{-1}$  to  $7.5 \text{ mL min}^{-1}$ . Therefore, it was concluded that protein adsorption does not depend on flow rate under the experimental conditions. This result is in accordance with the Langmuir theory, in which protein adsorption depends on the protein concentration and the type of substrate only.

### 3.5 Adsorption Isotherm and Calculation of Monolayer Coverage

The adsorption isotherm for adsorption of BSA and  $\gamma$ -globulin on Hydrosart and CN membranes was measured for stabilized protein formulations containing 0.01 % PS80. With this surfactant concentration, protein adsorption was reversible as discussed above. The protein concentration was varied in the range of  $0.1 \text{ g L}^{-1}$  up to  $5 \text{ g L}^{-1}$ . For  $\gamma$ -globulin the UV-signal was linear only for a protein concentration up to  $2 \text{ g L}^{-1}$ . Therefore, no higher concentration could be measured. Measurements were performed at a flow rate of  $0.9 \text{ mL min}^{-1} \text{ cm}^{-2}$ . The degree of adsorption was similar for both proteins and membranes due to the presence of the surfactant.

The resulting adsorption isotherm for BSA and  $\gamma$ -globulin is presented in Fig. 10. A Langmuir regression was included in the figure in the measured concentration range up to  $5 \text{ g L}^{-1}$ . Only a slight deviation from a linear plot can be observed at  $5 \text{ g L}^{-1}$  for BSA. Results are nearly independent of type of protein and type of membrane.

The coverage of the membrane surface is calculated first based on the given membrane properties. In literature the weight of a monolayer BSA on a surface is given with  $150 \text{ ng cm}^{-2}$ – $200 \text{ ng cm}^{-2}$  [21]. The  $\gamma$ -globulin monolayer is given at saturation with  $1.1 \pm 0.1 \text{ pmol cm}^{-2}$  surface area [22], assuming a protein weight of  $150 \text{ kDa}$ , this equals  $150$ – $180 \text{ ng cm}^{-2}$ . The surface of a membrane material can be calculated by measurement of the BET surface with nitrogen and the mass per unit area of a specific material (Tab. 1).

Resulting coverage values are summarized in Tab. 4. The values are quite comparable concerning the different proteins. According to the calculation a monolayer coverage in the range of  $91$ – $112 \text{ µg cm}^{-2}$  can be expected for protein adsorption on CN membranes compared with values between  $52$ – $69 \text{ µg cm}^{-2}$  for protein adsorption on Hydrosart membranes. The BET surface and the mass per unit area are both measured for the dry material. Therefore, it can be assumed that in the wet state the surface of the Hydrosart membrane is significantly enlarged due to the swelling properties of cellulose and more protein is needed to obtain a monolayer coverage.

Calculation of the monolayer coverage based on a fit of the adsorption isotherm (Fig. 10) using the Langmuir equation leads to unrealistic high values of  $4.8 \cdot 10^3 \text{ µg cm}^{-2}$  for BSA and  $6.7 \cdot 10^6 \text{ µg cm}^{-2}$  for  $\gamma$ -globulin with standard deviations exceeding the actual calculated value.

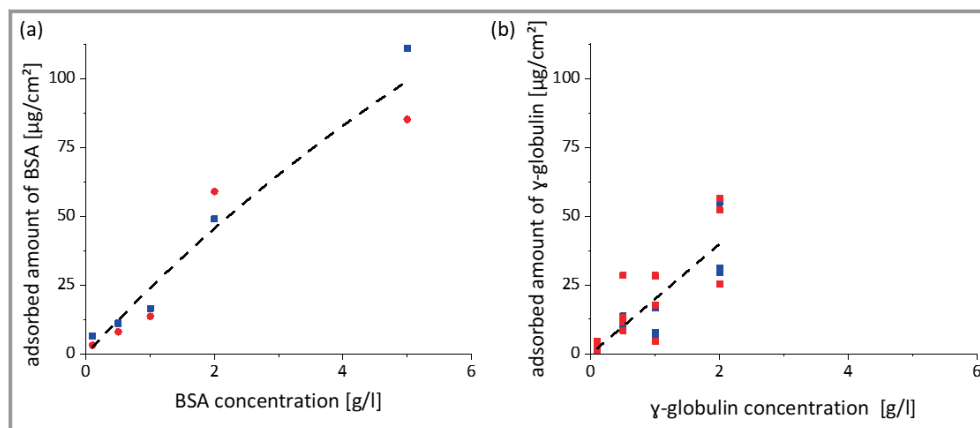


**Figure 10.** Adsorption isotherm according to the measured adsorption data for adsorption of BSA and  $\gamma$ -globulin during filtration of protein formulation containing 0.01 % PS80 through Hydrosart (blue) and CN (red) with theoretically calculated Langmuir regression (black, dashed lines).

**Table 4.** Comparison of calculated monolayer coverage based on literature and BET-measurements and measured equilibrium coverage  $m_{eq}$  as calculated according to Eq. (14) for adsorption of BSA and  $\gamma$ -globulin during filtration of protein formulations (Tabs. 2 and 3 containing 0.01 % PS80 through Hydrosart and CN membranes (0.2  $\mu$ m nominal pore size)).

Membrane	Hydrosart	CN
BSA monolayer calculated [ $\mu\text{g cm}^{-2}$ ]	52–69	91–122
BSA $m_{eq}$ measured by ILC [ $\mu\text{g cm}^{-2}$ ]	$52 \pm 6$	$36 \pm 6$
$\gamma$ -globulin monolayer calculated [ $\mu\text{g cm}^{-2}$ ]	52–62	91–109
$\gamma$ -globulin $m_{eq}$ measured by ILC [ $\mu\text{g cm}^{-2}$ ]	$28 \pm 4$	$34 \pm 5$

Finally, the following approach was used to calculate the coverage of the membrane surface on the basis of the measured adsorption values in Fig. 10. It cannot be assumed that the adsorption process leads to a homogeneous coverage of the membrane surface. Therefore, an equilibrium coverage,  $m_{eq}$ , is calculated instead of a monolayer, but still based on the Langmuir equation (Eq. (1)). The surface coverage  $\theta$  of the Langmuir equation is replaced by the ratio of the adsorbed amount of protein  $m_{ads}$  (measured after filtration of 40 mL of protein solution) and the equilibrium coverage  $m_{eq}$ :

$$\frac{m_{ads}}{m_{eq}} = \frac{Kc}{1 + Kc} \quad (12)$$

The adsorbed amount of protein  $m_{ads}$  can be measured, the protein concentration in the test solution is known, and the constant  $K$  can be calculated according to Eq. (13) using the kinetic information of the experimental results:

$$K = \frac{k_{ad}}{k_{de}} \quad (13)$$

The parameters  $k_{ad}$  and  $k_{de}$  are the adsorption and the desorption rate. Both can be determined by calculation of the first derivative of the adsorption measurements and determination of the maximum of the adsorption rate ( $k_{ad}$ ) and the minimum of the desorption rate ( $k_{de}$ ). The adsorption and desorption rates are presented in Fig. 11.

Maximum adsorption and desorption rates in dependence on protein concentration are summarized in Fig. 12 for formulations containing 0.01 % PS80. At the beginning of the filtration of protein solution through the membrane, the whole surface is still available, and no desorption occurs. Therefore, it can be assumed that the measured adsorption rate is here equal to the adsorption rate constant. For calculation of the desorption rate a similar approach can be used for the desorption process: the maximum of the absolute value of the desorption rate at the beginning of the desorption process is equal to the desorption rate constant. With  $k_{ad}$  and  $k_{de}$  first the constant  $K$ , and with this the equilibrium mass  $m_{eq}$  are calculated using Eqs. (12) and (13).

It can be seen from Fig. 12 that for both membranes adsorption and desorption rate are quite similar. Therefore, the constant  $K$  is averaged for both membrane types. For  $\gamma$ -globulin a constant  $K_{\gamma\text{-globulin}}$  of 1.02 and for BSA a constant  $K_{BSA}$  of 0.98 is obtained.

$$m_{eq} = \frac{m_{ads}(1 + Kc)}{Kc} \quad (14)$$

Now the equilibrium coverage can be calculated according to Eq. (14). Fig. 13 summarizes the results for the studied protein formulations. The resulting  $m_{eq}$  values are quite comparable for both proteins studied and quite independent of the protein concentration.

The obtained equilibrium coverage,  $m_{eq}$  (according to Eq. (14)), are compared with the coverage of the membrane surface as calculated above based on the measured membrane properties. The results are summarized in Tab. 4.

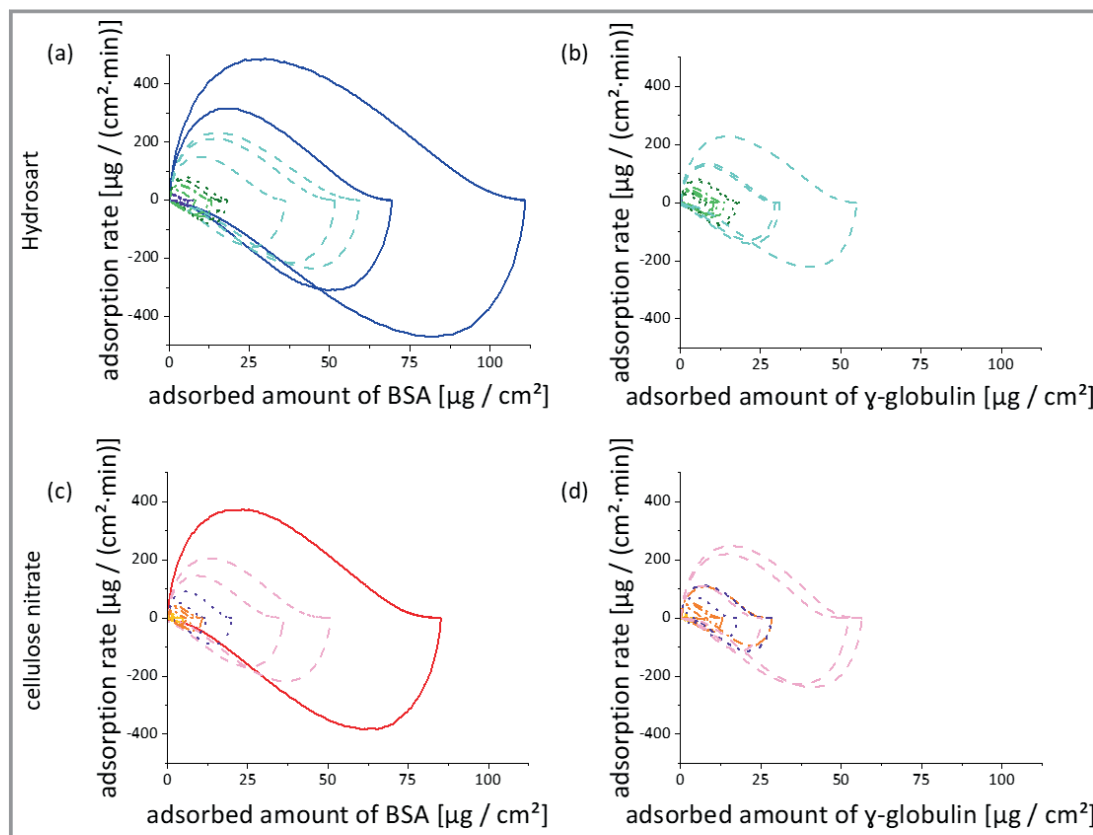


**Figure 11.** Adsorption and desorption rates for the multiple measurement cycles presented in Fig. 10 for BSA (a and c) and  $\gamma$ -globulin (b and d) formulations containing 0.01 % PS80. 5 g L<sup>-1</sup> (blue and red, straight lines), 2 g L<sup>-1</sup> (cyan and rose, dashed lines), 1 g L<sup>-1</sup> (olive and lilac, dotted lines), 0.5 g L<sup>-1</sup> (green and orange, dotted and dashed lines) and 0.1 g L<sup>-1</sup> (yellow and lilac, short dashed lines).

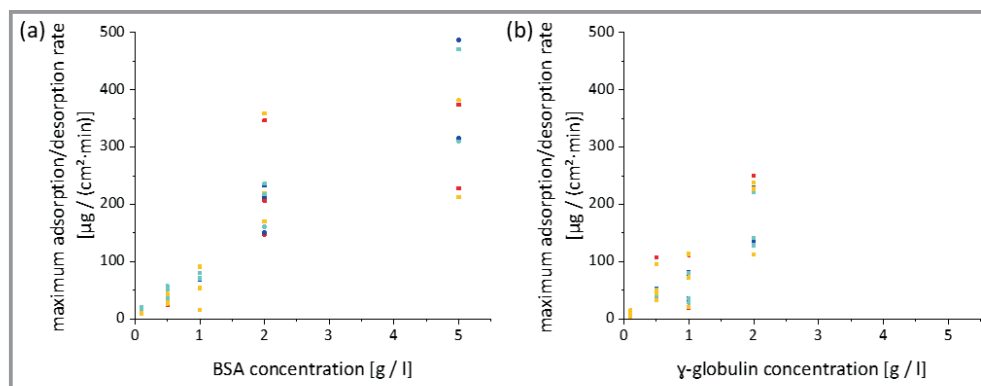


**Figure 12.** Maximum adsorption and desorption rates for a) BSA and b)  $\gamma$ -globulin during filtration of protein formulations through Hydrosart and CN membranes (0.2  $\mu\text{m}$  nominal pore size), calculated by deviation of the measured protein adsorption.

A good agreement was obtained for the calculated monolayer and the equilibrium mass  $m_{\text{eq}}$  for protein adsorption on hydrophilic Hydrosart membrane surface. Comparable values  $m_{\text{eq}}$  were obtained for protein adsorption on hydrophobic CN membranes, which are smaller than the calculated monolayer. This can be explained with the presence of the surfactant in the protein formulations. Surfactants cover all surfaces and turn them hydrophilic. Therefore,  $m_{\text{eq}}$  values are well comparable and independent of the type of substrate.

Compared with the determined  $m_{\text{eq}}$  values, the adsorption isotherm in Fig. 10 reaches higher adsorbed amounts of BSA for protein concentration  $> 2 \text{ g L}^{-1}$ . This can be explained by either the extent of the covered surface is enlarged, or multilayers are formed. Comprehensive study of filtration of stabilized (by PS80) protein formulation was performed in parallel (results not shown). [23]

Protein concentration was varied between 2 and 200 g L<sup>-1</sup>. Even high concentrated protein formulations could be

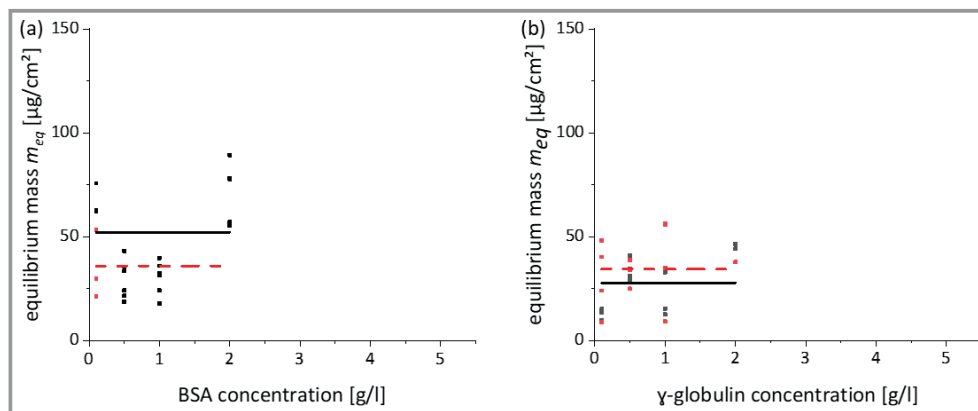


**Figure 13.** Calculated equilibrium mass  $m_{eq}$  according to Eq. (14) for adsorption of BSA and  $\gamma$ -globulin during filtration of protein formulations (Tabs. 2 and 3) containing 0.01 % PS80 through Hydrosart (black squares) and CN (red squares) membranes, both membranes with  $0.2 \mu\text{m}$  nominal pore size. Average values for Hydrosart (black, straight line) and CN (red, dashed lines).

filtered without significant filter fouling through hydrophilic and hydrophobic microfilter membranes. Therefore, it can be assumed that adsorption of proteins during filtration from stabilized protein formulations is limited to the magnitudes measured in this study.

Finally, the impact of protein adsorption on product loss during filtration of a protein formulation is assessed using a production example that can be found in the literature [3]. According to this, a redundant sterile filtration setup was described with in total five separate filtration processes. About  $10 \text{ cm}^2$  filtration area were needed per liter filtrate. The final product concentration is given with  $75 \text{ g L}^{-1}$ . Assuming an adsorption of  $50 \mu\text{g cm}^{-2}$  (Tab. 4) for each of those five filtration steps, 0.003 % of the protein would be retained by adsorption to the membrane.

Manufacturing of a less stable protein formulation without a surfactant would lead to a significantly higher product loss as can be seen in Sect. 3.2. This has to be considered during the manufacturing of protein formulations, as here the formulation is not stabilized and numerous filtration steps are made.

No further modeling of protein adsorption with the two-state model was undertaken because of the limited amount of data. Based on our results, we assume that the transition of the reversibly to the irreversibly bound protein depends on the hydrophobicity of the substrate. The transition happens fast and the protein turns the surface hydrophilic in the process.

## 4 Summary

Protein adsorption during microfiltration processes was successfully studied by inverse liquid chromatography (ILC). According to the results, protein adsorption during filtration of protein formulations through microfilter membranes can be controlled by surfactants. A surfactant covers the membrane surface and changes its surface properties. For formulations containing a nonionic surfactant (PS80) in a concentration above the CMC, protein adsorption is reversible and occurs to a minimum degree independent of the surface

properties of the studied membrane. Adsorption in the range of  $15 \mu\text{g cm}^{-2}$  was measured for a protein concentration of  $1 \text{ g L}^{-1}$  BSA or  $\gamma$ -globulin at a flow rate of  $0.9 \text{ mL min}^{-1} \text{ cm}^{-2}$ .

Adsorption during filtration of surfactant-free protein formulations depends on the surface properties of the microfilter membrane. Low and reversible protein adsorption was found for filtration through hydrophilic Hydrosart membranes.

Strong and irreversible adsorption processes occur in case of filtration of protein formulations through hydrophobic microfilter membranes. This irreversible adsorbed protein layer can be thicker than a monolayer. Remaining protein covers the surface and renders it hydrophilic, afterwards adsorption is minimized again and at the same level as in case of a surfactant-containing formulation.

The adsorption isotherm was measured in case of reversible protein adsorption for protein formulations containing 0.01 % PS80. Modeling an equilibrium coverage,  $m_{eq}$ , for protein adsorption was performed on the basis of a modified Langmuir equation using the quotient between the adsorbed amounts of protein  $m_{ads}$  and an equilibrium coverage  $m_{eq}$  to describe the surface coverage  $\theta$  and using experimental determined adsorption and desorption rates to describe  $K$ . Resulting values were in the range of  $30 < m_{eq} < 50 \mu\text{g cm}^{-2}$  for both proteins studied independent on type of substrate, which is in good agreement with the expected monolayer coverage in case of protein adsorption on Hydrosart membranes.

Validation guides for qualification of filter products for filtration in biopharma production usually recommend performing adsorption studies to assess the adsorptive properties of the membrane. According to our results, those studies should be performed related to the respective application conditions, especially the composition and concentration of the formulation. Furthermore, those studies should be extended to the adsorptive properties of the housing material of the filter and all the other single-use plastic materials. All these materials are hydrophobic and often have a very rough surface, which facilitates protein adsorption.

## Symbols used

$c$	$[\text{g L}^{-1}]$	solute concentration
$c^*$	$[\text{g L}^{-1}]$	minimum solute concentration needed to exceed monolayer coverage (BET theory)
$k_{\text{ad}}$	$[\text{s}^{-1}]$	adsorption rate constant
$k_1^{\text{ad}}$	$[\text{s}^{-1}]$	adsorption rate for molecule in state 1
$k_2^{\text{ad}}$	$[\text{s}^{-1}]$	adsorption rate for molecule in state 2
$k_{\text{de}}$	$[\text{s}^{-1}]$	desorption rate constant
$k_1^{\text{de}}$	$[\text{s}^{-1}]$	desorption rate for molecule in state 1
$k_2^{\text{de}}$	$[\text{s}^{-1}]$	desorption rate for molecule in state 2
$k_{1 \rightarrow 2}^{\text{trans}}$	$[\text{s}^{-1}]$	transition rate for molecule in state 1 changing into state 2
$k_{2 \rightarrow 1}^{\text{trans}}$	$[\text{s}^{-1}]$	transition rate for molecule in state 2 changing into state 1
$K$	$[-]$	constant according to Langmuir theory
$L$	$[\text{g}]$	adsorbed amount of solute according to the BET theory
$L_{\text{mono}}$	$[\text{g}]$	adsorbed amount of solute to achieve a monolayer coverage according to the BET theory
$z$	$[-]$	constant for BET theory

## Greek letters

$\theta$	$[-]$	surface coverage
$\theta_1$	$[-]$	surface coverage due to molecules in state 1
$\theta_2$	$[-]$	surface coverage due to molecules in state 2
$\theta_j$	$[-]$	saturation coverage according to the random sequential adsorption model
$\Phi$	$[-]$	available surface function according to the random sequential adsorption model

## Abbreviations

BET	Brunauer, Emmet and Teller
BSA	bovine serum albumin

CN	cellulose nitrate
ILC	inverse liquid chromatography
PS80	polysorbat 80

## References

- [1] M. C. Manning, D. K. Chou, B. M. Murphy, R. W. Payne, D. S. Katayama, *Pharm. Res.* **2010**, *27* (4), 544–575.
- [2] S. J. Kapp, I. Larsson, M. van de Weert, M. Cárdenas, L. Jorgensen, *J. Pharm. Sci.* **2015**, *104* (2), 593–601.
- [3] CMC Biotech Working Group, *A-Mab: a Case Study in Bioprocess Development*, **2009**.
- [4] J.-H. Kim, J.-Y. Yoon, *Encyclopedia of Surface and Colloid Science*, 1st ed., Marcel Dekker, New York **2002**.
- [5] H. Ye, L. Huang, W. Li, Y. Thang, L. Thao, Q. Xin, S. Wang, L. Lin, X. Ding, *PSC Adv.* **2017**, *7*, 21398–21405.
- [6] T. Bialopiotrowicz, P. Blanpain, F. René, M. Lalande, *Ars Separatoria Acta* **2002**, *1*, 111–137.
- [7] K. Nakanishi, T. Sakiyama, K. Imamura, *Biosci. Bioeng.* **2001**, *91* (3), 233–244.
- [8] K. L. Jones, C. R. O. Melia, *J. Memb. Sci.* **2000**, *165*, 31–46.
- [9] J. D. Andrade, V. Hlady, *Adv. Polym. Sci.* **1986**, *79*, 1–63.
- [10] Saiful, Z. Borneman, M. Wessling, *J. Memb. Sci.* **2006**, *280*, 406–417.
- [11] K. Nakamura, K. Matsumoto, *J. Memb. Sci.* **2006**, *285*, 126–136.
- [12] A. Shiosaki, M. Goto, T. Hirose, *J. Chromatogr. A* **1994**, *679* (1), 1–9.
- [13] Ø. Halskau, A. Muga, A. Martinez, *Curr. Protein Pept. Sci.* **2009**, *10* (4), 339–359.
- [14] H. Yang, M. R. Etzel, *Ind. Eng. Chem. Res.* **2003**, *42* (4), 890–896.
- [15] R. A. Latour, *J. Biomed. Mater. Res. A* **2015**, *103* (3), 949–958.
- [16] S. J. Kapp, I. Larsson, M. Van De Weert, M. Cárdenas, L. Jorgensen, *J. Pharm. Sci.* **2015**, *104*, 593–601.
- [17] P. Schaaf, J. Talbot, *J. Chem. Phys.* **1989**, *91*, 4401–4409.
- [18] M. Rabe, D. Verdes, S. Seeger, *Adv. Colloid Interfac.* **2011**, *162* (1–2), 87–106.
- [19] B. A. Kerwin, *J. Pharm. Sci.* **2008**, *97* (8), 2924–2935.
- [20] <https://bitesizebio.com/32181/proteins-adsorbing-labware/> (accessed July 10, 2019)
- [21] B. Jachimska, K. Tokarczyk, M. Iapczyńska, A. Puciul-Malinowska, S. Zapotoczny, *Colloids Surf., A* **2016**, *489*, 163–172.
- [22] W. Liao, F. Wei, M. X. Qian, X. S. Zhao, *Sens. Actuator, B* **2004**, *101*, 361–367.
- [23] S. Haindl, *Basic Studies for Sterile Filtration Processing of Therapeutic Protein Formulations*, PhD Thesis, Universität Hannover **2020**.